Title
Label-free enrichment of fate-biased human neural stem and progenitor cells

Authors
Adams, Tayloria NG
Jiang, Alan YL
Mendoza, Nicolo S
et al.

Publication Date
2020-03-01

DOI
10.1016/j.bios.2019.111982

Peer reviewed

HHS Public Access

Author manuscript

Biosens Bioelectron. Author manuscript; available in PMC 2022 February 21.

Published in final edited form as:

Biosens Bioelectron. 2020 March 15; 152: 111982. doi:10.1016/j.bios.2019.111982.

Label-free enrichment of fate-biased human neural stem and progenitor cells

Tayloria N.G. Adams[a,c,d,*], **Alan Y.L. Jiang**[b,c,d], **Nicolo S. Mendoza**[c,d], **Clarissa C. Ro**[c,d], **Do-Hyun Lee**[b], **Abraham P. Lee**[b], **Lisa A. Flanagan**[b,c,d,e,**]

[a]Department of Chemical and Biomolecular Engineering, University of California, Irvine, Irvine, CA, 92697-2580, USA

[b]Department of Biomedical Engineering, University of California, Irvine, Irvine, CA, 92697-2627, USA

[c]Department of Neurology, University of California, Irvine, Irvine, CA, 92697-6750, USA

[d]Sue & Bill Gross Stem Cell Research Center, University of California, Irvine, CA, 92697-1705, USA

[e]Department of Anatomy & Neurobiology, University of California, Irvine, Irvine, CA, 92697-4291, USA

Abstract

Human neural stem and progenitor cells (hNSPCs) have therapeutic potential to treat neural diseases and injuries since they provide neuroprotection and differentiate into astrocytes, neurons, and oligodendrocytes. However, cultures of hNSPCs are heterogeneous, containing cells linked to distinct differentiated cell fates. HNSPCs that differentiate into astrocytes are of interest for specific neurological diseases, creating a need for approaches that can detect and isolate these cells. Astrocyte-biased hNSPCs differ from other cell types in electrophysiological properties, namely membrane capacitance, and we hypothesized that this could be used to enrich these cells using dielectrophoresis (DEP). We implemented a two-step DEP sorting scheme, consisting of analysis to define the optimal sorting frequency followed by separation of cells at that frequency, to test whether astrocyte-biased cells could be separated from the other cell types present in hNSPC cultures. We developed a novel device that increased sorting reproducibility and

[*]Corresponding author. University of California Irvine, 916 Engineering Tower, Irvine, CA, 92697-2580, USA. [**]Corresponding author. University of California Irvine 3030 Gross Hall 845 Health Science Road Irvine, CA, 92697-1705, USA. tayloria@uci.edu (T.N.G. Adams), lisa.flanagan@uci.edu (L.A. Flanagan).

Declaration of competing interest

The authors declare that they have no known competing financial interests or personal relationships that could have appeared to influence the work reported in this paper.

CRediT authorship contribution statement

Tayloria N.G. Adams: Writing - original draft, Writing - review & editing, Data curation, Formal analysis, Investigation, Methodology. **Alan Y.L. Jiang:** Writing - original draft, Writing - review & editing, Data curation, Formal analysis, Investigation, Methodology. **Nicolo S. Mendoza:** Data curation, Formal analysis, Investigation, Methodology. **Clarissa C. Ro:** Data curation. **Do-Hyun Lee:** Writing - review & editing. **Abraham P. Lee:** Writing - review & editing. **Lisa A. Flanagan:** Writing - original draft, Writing - review & editing, Formal analysis, Methodology.

Appendix A. Supplementary data

Supplementary data to this article can be found online at https://doi.rg/10.1016/j.bios.2019.111982.

provided both enriched and depleted cell populations in a single sort. Astrocyte-biased cells were successfully enriched from hNSPC cultures by DEP sorting, making this the first study to use electrophysiological properties for label-free enrichment of human astrocyte-biased cells. Enriched astrocyte-biased human cells enable future experiments to determine the specific properties of these important cells and test their therapeutic efficacy in animal models of neurological diseases.

Keywords

Cell sorting; Dielectrophoresis; Membrane capacitance; Microfluidic; Neural stem and progenitor cell; Astrocyte

1. Introduction

Human neural stem and progenitor cells (hNSPCs) possess regenerative properties; as undifferentiated cells they secrete factors beneficial for cell survival and function and upon differentiation they form the mature cells of the central nervous system (astrocytes, neurons, and oligodendrocytes). HNSPC cultures expanded for therapeutic purposes are heterogeneous, containing stem cells, partially differentiated progenitors, and fully differentiated cells. HNSPC transplants improve functional recovery in animal models of a wide array of neurological conditions, such as amyotrophic lateral sclerosis (ALS), stroke, and Alzheimer's disease (Lindvall and Kokaia, 2006). Based on positive preclinical findings, many clinical trials are underway with hNSPCs.

The cells in most transplantation studies are unsorted, heterogeneous hNSPCs. However, many neurological conditions could benefit from transplantation of a more targeted cell population. For example, an astrocyte deficiency in ALS patients could be remedied by a cell therapy approach to replace the defective cells (Lepore et al., 2008; Yamanaka and Komine, 2018). HNSPC cultures contain cells destined to form astrocytes, but little is known about the defining characteristics of astrocyte-biased cells, making it difficult to obtain enriched populations of these cells for therapeutic purposes. A method to rapidly identify and enrich human cells that will form astrocytes would advance stem cell therapeutics for human disease.

We found specific electrophysiological properties identify hNSPC populations that are biased toward forming either astrocytes or neurons, potentially creating a novel means for isolating astrocyte-biased human cells (Labeed et al., 2011). An electrophysiological property, whole cell membrane capacitance (C_{mem}), indicates the eventual fate of hNSPCs; astrocyte-biased hNSPCs have higher membrane capacitance values while neuron-biased hNSPC membrane capacitance values are lower (Labeed et al., 2011). The fate-specific differences in membrane capacitance are evident in undifferentiated hNSPCs, meaning that the ability of the cells to form astrocytes can be detected prior to their differentiation and expression of known astrocyte markers. Membrane capacitance distinguishes lineage specification in other stem cell types, showing that membrane electrophysiological measures are valuable indicators of cell fate in many stem cell lineages (Vykoukal et al., 2009; Bagnaninchi and Drummond, 2011; Song et al., 2015; Lee et al., 2018a). Cell-type specific

membrane capacitance values could provide a new avenue for enriching human astrocyte-biased cells.

Whole cell membrane capacitance can be measured by dielectrophoresis (DEP). DEP is a label-free technique that uses electric field gradients to analyze and separate cells based on the electrophysiological properties of the plasma membrane and cytoplasm. DEP has been applied to a wide variety of cell types such as red blood cells (Srivastava et al., 2008; Leonard and Minerick, 2011), white blood cells (Khoshmanesh et al., 2011), cancer cells (Salmanzadeh et al., 2012), and yeast (Patel et al., 2012; Razak et al., 2013). Additionally, studies of the NCI-60 panel of human tumor cells and ovarian cancer cells show that cells of similar size with different membrane features (i.e. membrane folding, surface roughness, etc.) can be characterized and isolated using DEP (Gascoyne et al., 2013; Salmanzadeh et al., 2013). Cell movement in DEP is used to calculate whole cell membrane capacitance. Cells in electric fields have distinct dielectric dispersions. At radio frequencies (β-dispersion region), 100 kHz to 10 MHz, and in low conductivity media (~100 μS/cm), DEP can be used to determine electrophysiological properties of the plasma membrane and cytoplasm. Within this frequency range, dielectric dispersions of spherical cells are dominated by the plasma membrane at lower frequencies while higher frequencies penetrate the cell surface to probe the cytoplasm (Martinsen et al., 2002; Adams et al., 2013, 2014). The distinct DEP responses of astrocyte- and neuron-biased hNSPCs are in the low frequency β-region (Labeed et al., 2011) and dominated by the plasma membrane.

DEP can be used to separate cells that differ in electrophysiological properties. Cells move in DEP due to Maxwell-Wagner interfacial polarizations that govern cell responses in the β-region. Polarized cells will display either positive DEP (pDEP), in which cells move to high electric field gradient areas, or negative DEP (nDEP), in which cells repel from high electric field gradient areas (Pethig, 2010). The electric field interacts with ions available in the medium causing them to align around the cell (interfacial polarization) (Chen and Pohl, 1974). The movement and alignment of ions on the outside of the cell are affected by the content and properties of the cell surface (Pohl, 1978). Thus, different cell surfaces will affect polarization in contrasting ways and cause cells to have distinct pDEP and nDEP responses. The induced DEP force that causes cell movement is given by $\vec{F}_{DEP} = 2\pi\varepsilon_{med}R^3Re[f_{CM}]\nabla\vec{E}_o^2$ (Pethig, 2010) where ε_{med} is the medium permittivity (F/m), R is the cell radius (μm), *Re[fCM]* is the real part of the Clausius-Mossotti factor (unitless) and describes cell motion in the electric field, and $\vec{E}_o$ is the electric field. The movement of cells in response to the applied electric field can be used to separate cells differing in membrane capacitance.

Alternating current (AC) DEP utilizes the frequency of the applied electric field to induce cell movement and separate cells. AC DEP spectra have two characteristic crossover frequencies (*fxo*) at which there is no net movement in response to the electric field since the cells display neither pDEP nor nDEP. The first *fxo* occurs at lower frequencies (typically between 10–100 kHz) and is determined by cell size, shape, and plasma membrane composition. The second, higher *fxo* is influenced by the cell cytoplasm and typically occurs at frequencies above 10 MHz in low conductivity media (Salmanzadeh and Davalos,

2014). The first *fxo*, along with other data points from the DEP spectra, is used to calculate membrane capacitance (Broche et al., 2005; Adams et al., 2014). HNSPCs that differ in fate also differ in the first *fxo* in AC DEP (Labeed et al., 2011), making it possible that DEP could be used to enrich astrocyte-biased cells from heterogeneous hNSPC populations.

We initially tested DEP-based sorting of NSPCs using mouse cells since mouse astrocyte-biased cells also have higher membrane capacitance values than their neuron-biased counterparts (Labeed et al., 2011). Astrocyte-biased mouse cells were enriched from a heterogneous population of NSPCs at lower frequencies in DEP (Nourse et al., 2014; Simon et al., 2014), consistent with their higher membrane capacitance values (Pethig et al., 2010). Based on these successful studies with mouse cells, we hypothesized that DEP could be used to enrich human astrocyte-biased cells relevant for therapeutic applications.

Sorting hNSPCs on the basis of their inherent electrophysiological properties would provide a number of significant advantages. DEP is ideal for cell sorting because it is a label-free, rapid, straightforward method capable of separating desired cell subpopulations from heterogeneous mixtures. The induced cell movement in DEP resulting from polarization in the electric field is utilized for cell separations, meaning that cells need not be labeled. This is an advantage since cell type specific markers are not always available and labeling cells with antibodies may change cell properties. The induced cell movement in DEP is very fast, occurring almost instantaneously. Coupled with the fact that cells need not be labeled prior to separation, this enables rapid isolation of cells of interest. Additionally, DEP-based sorting is easily adaptable to a clinical setting since DEP devices do not require complicated equipment for cell separation and the devices are easy to sterilize. DEP can thus be used as a point of care separation technology for human cells. DEP parameters can be optimized to ensure the electric fields are not harmful to NSPCs (Lu et al., 2012). Short-term electric field exposure (1 min or less) at all DEP frequencies does not affect hNSPC survival, proliferation, or differentiation (Lu et al., 2012). HNSPCs exposed to electric fields at any frequency for up to 30 min showed no effects on either cell proliferation or differentiation (Lu et al., 2012). However, cell death was observed near the *fxo* when the electric field exposure time was 10 to 30 min (Lu et al., 2012). Therefore, short exposure times should be used when using frequencies near the *fxo* for sorting hNSPCs. This is easily achievable since DEP induces rapid movement of cells (on the order of seconds).

We tested whether astrocyte-biased cells with potential clinical relevance could be enriched from a heterogeneous population of hNSPCs. We utilized two different microfluidic DEP sorting devices (microwell device and hydrophoretic oblique angle parallel electrode sorting device), tested whether a pre-sorting analysis could predict the optimal sorting frequency, and analyzed the DEP spectra, membrane capacitance values, and astrocyte differentiation of the sorted cells.

2. Materials and methods

2.1. Cell culture and preparation for DEP

Fetal brain-derived hNSPCs (SC27) isolated from the cerebral cortices of autopsy brain were maintained in proliferation media as previously described (Schwartz et al., 2003; Flanagan

et al., 2006). All hNSPC cultures were maintained in a humidified incubator, operating at 37 °C with 5% CO_2, until the DEP experiment. Experiments utilized hNSPC cultures at passages 14–19.

HNSPCs were dissociated into a single cell suspension for DEP experiments using non-enzymatic Cell Dissociation Buffer (Invitrogen, Carlsbad, CA). Dissociated cells were washed three times with and resuspended in a DEP buffer solution, an iso-osmotic medium consisting of 8.5% (w/v) sucrose, 0.3% (w/v) glucose with final conductivity adjusted to 100 μS/cm using 0.7% (w/v) RPMI-1640. The conductivity was measured with a conductivity meter (Thermo Orion, Beverly, MA). An alternative DEP buffer solution consisting of PBS with calcium and magnesium (0.1 mM Ca and 0.25 mM Mg) (Fry et al., 2012) was also tested. For sorting with the hydrophoretic oblique angle parallel electrode sorting (HOAPES) device, resuspended cells were filtered with 35 μm nylon mesh cell strainer tubes to remove any cell clumps. The final cell concentration was adjusted to ~2×10^6 cells/mL (microwell device) and ~3×10^6 cells/mL (HOAPES device).

2.2. Pre-sort analysis to determine optimal sorting frequency

The optimal sorting frequency was determined with two methods. In one, cells were loaded in the microwell device and frequencies scanned between 10–1000 kHz. The number of cells attracted to the electrode edges (pDEP) was counted and expressed as a percentage of the total cells. A trapping curve was then constructed showing the percentage of cells experiencing pDEP at each frequency. The second method used a 3DEP analyzer (LabTech, East Sussex, UK) (Broche et al., 2005) to characterize the DEP spectrum from 2–20,000 kHz for heterogeneous hNSPCs prior to sorting (referred to as “presort”). The DEP spectrum was translated to a trapping curve based on cells experiencing pDEP (% cell pDEP) by normalizing the intensity data, % cell pDEP = $I_{AVG} - I_{MIN} = I_{MAX} - I_{MIN}$. The 3DEP analyzer was also used to measure whole cell membrane capacitance. The whole cell membrane capacitance was estimated using the single-shell spherical DEP polarization model included in the 3DEP analyzer software.

2.3. hNSPC sorting with microwell device

The microwell device was prepared for sorting by treating for 30 min with UV light in the cell culture hood to sterilize. Then, the device was washed 3 times with 70% ethanol, followed by sterile H_2O and then DEP buffer, using 120 μL of each solution in each well. HNSPCs were sorted at the target frequency for less than 5 min in the microwell device using methods previously described for mouse NSPCs (Simon et al., 2014; Adams et al., 2018). Control cell populations included cells grown in regular hNSPC media (media control), cells incubated in DEP buffer for the duration of the sorting experiment (DEP buffer control), and cells in DEP buffer placed in the device but exposed to 1 MHz frequency at which all cells experience pDEP, so no sorting occurs (1 MHz control). At the end of each sort, 20K cells from each condition (controls and sorted cells) were evenly plated onto 12 mm laminin coated coverslips in proliferation media. Cell enrichment was assessed based on post-sort analysis of DEP spectra and membrane capacitance with the 3DEP analyzer and hNSPC differentiation and immunostaining to measure astrocyte formation (described below).

2.4. Hydrophoretic Oblique Angle Parallel Electrode Sorting (HOAPES) device design and fabrication

The HOAPES device is a continuous DEP-based cell sorter comprised of three main sections: filter, sheathless hydrophoretic cell aligner, and oblique parallel electrodes adapted from an earlier design (Lee et al., 2018b). There is a single 1.5 mm diameter inlet directly followed by an array of 30 μm tall PDMS posts to create a filter to capture cell clumps. The sheathless hydrophoretic cell aligner section is 500 μm wide with an array of 40 μm thick ridged microstructures embedded in a serpentine channel all created with PDMS. The oblique parallel electrodes are angled at 45° and form a V-shape. Electrodes are 35 μm in width with 35 μm gaps between them. At the end of the channel there are 8 μm wide perforated trifurcations between 3 outlet microchannels (one middle and two outer) with 1.5 mm diameter outlets.

The electrodes were fabricated using standard photolithography techniques previously described (Simon et al., 2014). Briefly, 200 Å titanium followed by 1000 Å gold were coated on standard 25 mm × 75 mm glass slides using electron-beam physical vapor deposition. The electrode features were transferred onto the gold coated slide using Shipley 1827 positive photoresist (Shipley Company, Marlborough, MA, USA).

The structure of the microchannels was created with two-step photolithography (Choi and Park, 2010). In the first step, a 30 μm thick layer of SU-8 2025 photoresist (MicroChem Corp., Newton, MA, USA) was spin coated onto a silicon substrate, the first layer photomask was manually aligned, and UV cured. In the second step, a 40 μm thick layer of photoresist was spin coated onto the first layer of photoresist and a second photomask was aligned to the first layer and cured using a mask aligner (Karl Suss MA6 Mask Aligner). PDMS was cast onto the mold, cured, and cut to the desired size. Inlet and outlets were punched in the PDMS using a 1.5 mm diameter biopsy punch.

To assemble the device, the PDMS substrate and the electrode slide were irreversibly bonded after a 2-min oxygen plasma treatment. Finally, 22-gauge solid copper wires were soldered onto the electrode pads for electrical connection.

2.5. hNSPC sorting with HOAPES device

The HOAPES device was placed on a hot plate set at 150 °C for 30 min to sterilize and remove moisture. Fluid flow to the device was driven by a syringe pump (Harvard Apparatus PicoPlus, Holliston, MA) pushing a 1 mL syringe with 1.5 mm outer diameter Tygon® tubing connected to the device inlet. To remove bubbles from the microchannels and sterilize, 70% ethanol was pumped into the device at 20 μL/min. Filtered MQ H_2O was then flowed into the device at 20 μL/min for 15 min to wash away all ethanol. Bovine serum albumin (BSA, 5%) diluted in filtered MQ H_2O was then washed through the device for 15 min at 10 μL/min to coat the walls of the microchannels, preventing cell sticking. BSA was washed away with 100 μS/cm DEP buffer at 20 μL/min for 15 min. The device was then mounted on an upright Olympus microscope (model BX41) with bright field objectives and connected to a function generator (AFG320, Tektronic, Beaverton, OR). A commercial

dSLR camera (Canon model EOS Rebel T2i) was attached to the microscope to record videos and monitor sorting.

Videos were used to highlight trajectories of hNSPCs moving through the device. Videos were stacked in ImageJ using standard deviation of the intensity (maps the change in intensity from one frame to another) to create images. Each stacked Z-projection image was generated from 30 s of video, and the signal intensity across the channel in each image was measured using ImageJ.

The fluid flow rate appropriate for cell sorting was determined by monitoring the flow profile of hNSPCs at a low concentration (1×10^6 cells/mL), slow flow rate (1 μL/min), and high frequency (~1 MHz) using 6 V peak to peak (Vpp). This frequency was chosen so the majority of the cells experienced pDEP and focused to the middle channel; we aimed for 95%. Then, the fluid flow rate was slowly increased to a maximum rate at which 95% of the cells remained focused to the middle channel. The optimal fluid flow rate was found to be 3.5 μL/min.

To optimize sorting, a pre-sort focusing curve was determined by counting the number of cells that focused to the center outlet divided by the total number of cells collected from the device at frequencies from 25 kHz to 1000 kHz using 6 Vpp and 3.5 μL/min flow rate. The frequency (f_1) at which 30% of the cells focused to the middle outlet was linearly interpolated from the focusing curve and used for sorting. HNSPC sorting was carried out in batches due to cell settling. In the beginning of each run, the syringe was primed with DEP buffer; there-after, 30 μL of cell solution was drawn into the tubing then inserted into the inlet. The electrodes were actuated at f_1 and the syringe pump turned on to induce flow of cells into the sheathless hydrophoretic cell aligner and oblique parallel electrode sections (6 Vpp and 3.5 μL/min flow rate). The accuracy of the predicted sorting frequency was checked by calculating the percentage of cells focused. For a sorting batch, the focused cells were collected from the middle channel and manually counted and then divided by the total number of cells collected from the device. In all sorts cells were exposed to electric fields for less than 5 min. At the end of each run, f_1 focused cells from the center outlet and f_1 unfocused cells from the outer outlets were collected and placed in separate Eppendorf tubes with proliferation media. Additional runs were completed at a second, control frequency, f_2, (1 MHz) in which the majority of the cells focused to the center outlet. If some cells remained unfocused, they were collected from the outer outlets and mixed with the focused cells; creating an unsorted control sample at f_2. Two other control samples were collected: cells that remained in proliferation media (media control) and cells that were incubated in the DEP buffer until the end of the sort (DEP buffer control). The flow profile before and after the electrode array was closely monitored to discard any runs with irregular flow due to cell clumps or debris. At the end of each sort, 15K cells from each condition (controls, f_1 focused, f_1 unfocused, f_2) were evenly plated onto 12 mm laminin coated coverslips in proliferation media. Cells were then differentiated and immunostained to assess astrocyte formation (described below).

2.6. hNSPC differentiation

To induce differentiation for cells sorted with the microwell device, hNSPC proliferation media was changed after 24 h to differentiation media (Neurobasal supplemented with 1X B27, 1X GlutaMax, 100 units/mL penicillin/streptomycin, 20 ng/mL BDNF, 20 ng/mL GDNF, and 0.5 μM dibutyryl cyclic AMP (cAMP; Sigma-Aldrich, St. Louis, MO, USA) (modified from (Yuan et al., 2011). For cells sorted with the HOAPES device the hNSPC proliferation media was replaced with differentiation media (DMEM/F12 + 20% BIT supplemented with 1X B27, 1X GlutaMax, 100 units/mL penicillin/streptomycin, 20 ng/mL BDNF, 20 ng/mL GDNF, and 0.5 μM cAMP) after 24 h. Both differentiation media allow formation of astrocytes and neurons. This enabled the nature of the sorted cells (i.e. whether they will form astrocytes) to be revealed without the media directing the cells to turn into a particular type of differentiated cell. Daily 50% media changes were maintained to facilitate cell differentiation. A 5-day differentiation period was carried out to assess astrocyte formation. After differentiation, cells were immunostained with anti-glial fibrillary acidic protein (anti-GFAP) polyclonal (Sigma Aldrich, Cat #G9269) at 1:1000 or monoclonal (Sigma Aldrich, Cat #G3893, clone GA5) at 1:400 and stained with secondary antibody (Alexa 288, Jackson ImmunoResearch) at 1:100 as previously described (Flanagan et al., 2008; Labeed et al., 2011). Cells counted as astrocytes exhibited typical astrocyte morphologies and a filamentous pattern of GFAP reactivity in the cytoplasm. Controls included cells stained with secondary antibodies only (negative controls) and appropriate subcellular localization of antibody signal (cytoskeletal for GFAP intermediate filament protein).

Cells were imaged with an inverted Nikon-TE fluorescent microscope. Three to five randomly selected fields for each 12 mm coverslip were selected for quantitation. From these fields, the number of GFAP-positive cells and the number of nuclei were counted using ImageJ. The percent GFAP-positive cells were calculated for each collected sample.

2.7. Statistical analysis

Statistical analysis was completed using One-Way ANOVA with Tukey post hoc test for multiple comparisons for samples with n = 3 or more biological replicates. Biological replicates are listed as “n” in figure legends.

3. Results and discussion

3.1. Defining optimal sorting frequency for hNSPCs

A key first step for sorting cells with AC DEP is to define the optimal frequency for sorting the desired cell population. We found previously that astrocyte-biased hNSPCs have higher membrane capacitance values and lower *fxo* than neuron-biased cells (Labeed et al., 2011). This suggests that astrocyte-biased cells can be sorted by their likelihood of experiencing pDEP at lower frequencies. We also previously found that astrocyte-biased mouse NSPCs can be enriched at lower frequencies where 30% of the cells experience pDEP (Nourse et al., 2014; Simon et al., 2014). Based on our previous sorting of mouse NSPCs, we targeted a low frequency for sorting hNSPCs at which 30% of the cells would experience pDEP.

We discovered that the DEP responses of hNSPCs were variable across different batches of cells and varying frequencies were required to achieve 30% pDEP for sorting. The variation in sorting frequency could be due to many factors including electrode aging from biofouling, changes in sample cellular composition (stem cells are dynamic), and/or cellular release of ions into the sorting buffer. We screened each set of hNSPCs prior to sorting to determine the frequency that gave 30% of the cells in pDEP for each batch of cells. Screening was initially performed manually by generating a pDEP trapping curve for the cell population. This was achieved by observing the behavior of cells in a DEP microwell device over a range of frequencies and quantifying the percentage of cells experiencing pDEP (cells trapped along the electrodes). However, this procedure was time-consuming, so we tested whether a more rapid DEP-based analysis could predict sorting frequencies.

We used the 3DEP analyzer to quickly (in approximately 10 min) obtain the characteristic DEP spectra for hNSPCs prior to sorting (Fig. 1A). We translated 3DEP spectra to pDEP trapping curves to allow comparison with the manually-derived curves obtained with the microwell device (see Methods “Pre-sort analysis to determine optimal sorting frequency”). The 3DEP prediction was compared to the manually-derived curve and found to give good agreement in the lower range of frequencies used for sorting (Fig. 1B). We tested whether the 3DEP system could be used to predict the sorting frequency for a different cell population, mouse NSPCs. Similar to the results with hNSPCs, the 3DEP spectra accurately predicted the trapping behavior of the cells in the microwell device (Figs. S1A and B). Since the 3DEP system provided rapid prediction of sorting frequencies, we used it to calculate the 30% trapping point for hNSPCs across multiple sorts and found the frequencies ranged from 10–25 kHz. This approach optimized the sorting parameters by taking into account any variability in the cell population or the device prior to each sort. Pre-screening each batch of cells prior to sorting increased sorting reproducibility.

We tested whether a DEP buffer solution containing divalent cations would be beneficial for hNSPC sorting since the presence of calcium and magnesium appeared to stabilize ion channel activity in myocytes during DEP measurements (Fry et al., 2012). However, hNSPC survival was lower in the divalent cation containing buffer (31% cell loss compared to 13% in our original DEP buffer solution after 4 hrs), so we carried out experiments with our usual DEP buffer solution lacking divalent cations.

3.2. Astrocyte-biased cells were enriched from hNSPCs using a microwell DEP device

After determining the optimal frequency, we sorted hNSPCs at that frequency in a DEP device to determine whether astrocyte-biased cells could be enriched from the heterogeneous starting population of hNSPCs. We used a DEP microwell device (Fig. 2A) to sort hNSPCs since this device is simple to operate and had been successfully used previously for cell sorting (Simon et al., 2014). Several controls were generated for each sort. Unsorted controls included cells placed in DEP buffer solution with no exposure to the electric field and cells exposed to the electric field at 1 MHz, which induced pDEP for all the cells so did not induce separation.

HNSPCs sorted by low frequency DEP were similar in size to unsorted controls but differed from controls in DEP spectra and membrane capacitance. Cell sizes of sorted and unsorted

hNSPCs were similar; the average radii were 7.1 μm buffer control, 7.0 μm 1 MHz control, and 7.1 μm sorted (Fig. 2B). A comparison of the pDEP trapping curves for sorted cells and unsorted controls showed that a higher percentage of sorted cells experienced pDEP at low frequencies (Fig. 2C). The same trend held true for mouse NSPCs sorted in the microwell device (Fig. S1C). These data indicate that sorting was successful at enriching populations of cells experiencing pDEP at lower frequencies. Sorting enriched cells that have higher membrane capacitance values: the average membrane capacitance of sorted cells was 18 mF/m^2, compared to 15 mF/m^2 for buffer controls and 16 mF/m^2 for 1 MHz controls (Fig. 2D). These data show that low frequency DEP sorting of hNSPCs yielded cells that differ in DEP responses and electrophysiological properties (membrane capacitance) but not size.

We tested whether human astrocyte-biased cells were enriched by DEP sorting by differentiating the sorted cells and staining for any astrocytes that were formed (using the astrocyte marker glial fibrillary acidic protein, GFAP). Sorted cells formed more astrocytes than unsorted controls; the average percentage of GFAP-expressing cells was 33% sorted cells, 18% buffer control, and 19% 1 MHz control (Fig. 2E and F). There was a 1.8-fold enrichment of astrocyte-biased hNSPCs relative to buffer controls after sorting. HNSPCs sorted in the microwell device showed increased astrocyte generation, establishing proof-of-concept that astrocyte-biased cells can be enriched from hNSPCs using DEP.

HNSPC sorting with the microwell device was variable (Fig. S2). Cells sort in DEP due to their differences in electrophysiological properties. Thus, successful DEP sorts can be defined as those that enrich cells differing in electrophysiological properties, in this case membrane capacitance. We used membrane capacitance to measure the outcome of DEP sorting and found the microwell device successfully generated an enriched cell population only ~30% of the time, which was not very efficient (Fig. S2). Sorts that did not produce cells differing in membrane capacitance also did not enrich astrocyte-biased cells (Fig. S2). We therefore developed a different type of DEP-based sorting device to improve reproducibility and enable statistical analysis of sorting efficacy.

3.3. Testing of an improved DEP sorting device (HOAPES device)

We developed a robust DEP-based sorting platform with better reproducibility and the ability to continuously sort cells to increase yield. The HOAPES microfluidic DEP device contains three main components: filter, sheathless hydrophoretic cell aligner, and oblique electrodes (Fig. 3A). The filter blocks large particles such as cell clumps from entering the separation chamber. The sheathless hydrophoretic cell aligner utilizes lateral pressure gradients created by ridges in the fluid channel to direct cells to the outer edges of the microchannel (Song and Choi, 2013). The ridges have angles that gradually shift along the channel so that cells are progressively pushed toward the channel walls. Cells along the channel wall enter the oblique electrode region for DEP-based cell separation. Electrodes are arranged in a chevron pattern such that cells experiencing pDEP are directed to the center of the channel (Hu et al., 2005; Lee et al., 2018b). At the channel outlets, arrays of 8 μm wide “mini”-microchannels perpendicular to the fluid flow link the outlet trifurcation. These microchannels improve the robustness of the sorter by mitigating the effect of clogging at the trifurcation so that fluid flow does not get shifted to a different outlet.

In the HOAPES DEP device, cells flow through the filter and cell aligner sections before encountering the oblique parallel electrodes for DEP-based separation. With the electric field applied, cells entering the electrode section will either remain unfocused (nDEP) and flow along the microchannel walls or focus (pDEP) along the electrodes toward the channel center. Unfocused cells exit the two outer microchannels and the focused cells exit the middle microchannel (Fig. 3B). The two sorted cell populations (focused middle microchannel and unfocused outer microchannels) are collected from the outlets for further analysis.

We tested whether the HOAPES DEP device would perform as expected by tracking the trajectories of hNSPCs moving through the device. Cells are randomly distributed in the filter (Fig. 3C, G) and chamber (Fig. 3D, H) regions but focused along the microchannel sidewall after the aligner region (Fig. 3E, I). With the electric field on and the frequency set to 800 kHz, most hNSPCs experience pDEP and are focused to the center of the channel (Fig. 3F, J). The applied frequency can be tuned to control the percentage of cells focused to the center of the channel in order to select for enrichment of different cell subpopulations. A video shows movement of hNSPCs through each region of the HOAPES DEP device (Movie S1).

Supplementary data related to this article can be found at https://doi.org/10.1016/j.bios.2019.111982.

The unique design of the HOAPES DEP device required development of a new sorting workflow (Fig. 4). Cells were prepared for sorting in DEP buffer as used for the microwell DEP device. Control cell pop- ulations were hNSPCs in regular growth media, hNSPCs in DEP buffer solution, and hNSPCs collected at a high frequency, f_2 (e.g. 1 MHz), that focused all cells (Fig. 4A). We revised the method for determining the appropriate sorting frequency since the constant fluid flow in the HOAPES DEP device could shift the sorting frequency due to the interaction of fluidic and induced DEP forces on the cells. We generated a focusing curve with fluid flow in the device by measuring the percentage of cells focused to the middle outlet of the device across a range of frequencies in order to select a sorting frequency (Fig. 5). As an example, light intensity analysis of the trajectories of one batch of hNSPCs in the device showed that a sorting frequency of 200 kHz would focus ~23% of the cells while a lower frequency of 25 kHz would collect ~9% and a higher frequency of 800 kHz ~68% of the cells (Fig. 5). In this example, 200 kHz would be chosen as the sorting frequency to focus a subset of the hNSPCs to the middle microchannel while the majority of the cells would exit the outer microchannels (Fig. 4A schematic, Fig. 5 A,C hNSPCs). The effect of fluid flow on the sorting frequency was evident because the frequencies used for sorting in the HOAPES DEP device ranged from 60–300 kHz, with a mean of 233 kHz, which was much higher than the frequencies used for sorting in the microwell DEP device (10–25 kHz). Table S1 summarizes the predicted sorting frequencies from the focusing curve to target 30% of cells experiencing pDEP and the actual percentage of cells focused to the middle channel of the HOAPES device.

3.4. Astrocyte-biased cells were enriched in the focused fraction and depleted from the unfocused fraction after sorting hNSPCs with the HOAPES DEP device

We sorted undifferentiated hNSPCs in the HOAPES DEP device at frequencies chosen from focusing curves and differentiated the cells after sorting to measure the generation of astrocytes (Fig. 6A). Immunostaining of differentiated cells with the astrocyte marker GFAP indicated more astrocyte-forming cells in the focused sample than in controls or the unfocused sample (Fig. 6B–D). The percentage of GFAP-expressing cells was quantified and showed a significant enrichment of cells that generated astrocytes in the focused sorted cell population compared to control unsorted cells (Fig. 6E). Astrocyte-producing cells were significantly depleted in the unfocused fraction (cells exited device through outer channels) compared to unsorted media controls (Fig. 6E). The unfocused cells had lower GFAP expression levels than the unsorted media control because the targeted astrocyte-biased cells were tracked to the middle outlet channel and thus depleted from the outer channels. The generation of both enriched and depleted astrocyte-biased cells in a single sort yields populations that differ more from each other than either sorted population compared to controls (Fig. 6E). There was no difference in the percentage of GFAP-positive cells differentiated from any of the control cell populations, showing that the conditions used for DEP sorting did not affect differentiation (Fig. S3). In support of this finding, we showed previously that conditions used for DEP did not change the differentiation potential of hNSPCs (Lu et al., 2012).

Our data show that astrocyte-biased populations of hNSPCs can be sorted using their inherent plasma membrane electrophysiological properties. Further, the HOAPES DEP device generates significantly enriched and depleted populations in a single sort, providing additional functionality not possible with our previous DEP sorting devices and enabling more robust downstream analysis of the function of human astrocyte-biased cells (Adams et al., 2018).

The operation of the HOAPES DEP device was much more reliable than that of the microwell device. Sorting hNSPCs with the HOAPES DEP device yielded enrichment in 5 out of 5 experiments, giving a success rate of 100%, which is much better than the 30% success rate of the microwell device (Fig. S2). We therefore achieved the goal of developing a more robust DEP sorter for hNSPCs.

3.5. Relevance for the field of stem cell sorting

This study, for the first time, shows the successful label-free isolation of a hNSPC subpopulation based on cell electrophysiological properties. Advantages to this approach include the fact that cells need not be labeled, which could alter cell function, and cells are not exposed to damaging high fluidic shear forces as found in fluorescence activated cell sorting (FACS). Pre-sorting analysis of the frequency response of cells in DEP was beneficial for improving sorting reproducibility.

Enrichment of cells isolated by lower frequency DEP sorting was demonstrated several ways. Firstly, a comparison of the DEP trapping curves of control and isolated cells showed that the sorted cell curve was shifted to lower frequencies (Figs. 2C and S1C). This indicates

that more of the cells in the sorted population experienced pDEP at lower frequencies, confirming that sorting enriched these cells. Secondly, membrane capacitance values were higher for sorted cells than controls (Fig. 2D), indicating that the sorting process selected cells that differ in this electrophysiological property. Finally, astrocyte-biased hNSPCs were enriched with two different DEP sorting devices (Figs. 2E, 6E). Rapid, label-free enrichment of astrocyte-producing human cells could advance stem cell therapeutics for human diseases such as ALS, where astrocytes are therapeutic cells of interest.

There was no difference in the size of sorted cells and controls (Fig. 2B), indicating that the enrichment of fate biased hNSPCs by DEP is not due to a difference between the size of these cells and others in the population. Similarly, there was no difference in the cell sizes of hNSPC populations that differ in fate (Labeed et al., 2011) and mouse NSPCs sorted on the basis of fate (Nourse et al., 2014). The differences in membrane capacitance values of astrocyte- and neuron-biased hNSPCs may be due to distinct patterns of glycosylation on the plasma membrane. We found that astrocyte/neuron fate of mouse NSPCs can be controlled by glycosylation (Nourse et al., 2014; Yale et al., 2018) and treatment of mouse NPSCs (Nourse et al., 2014; Yale et al., 2018) or hNSPCs (not shown) with an agent that shifts cell surface glycosylation significantly changes whole cell membrane capacitance. Plasma membrane glycosylation affects membrane structure and surface area, which could affect whole cell membrane capacitance and behavior in DEP (Wang et al., 1994; Gascoyne et al., 2013). Glycosylation impacts membrane microdomains such as microvilli and lipid rafts associated with membrane invaginations, and thus could lead to changes in membrane surface area not visible by phase contrast microscopy (Zhao et al., 2002; Garner and Baum, 2008). The cell surface glycocalyx, which is made up of glycoproteins, glycolipids, and galectins, creates thickened membrane regions that may affect capacitance and DEP responses (Paszek et al., 2014). Future studies will explore glycosylation as a potential underlying mechanism that could be responsible for the differences in membrane capacitance that enable enrichment of astrocyte-biased hNSPCs by DEP.

The sorting approach described here could be applied to many stem cell types, since membrane capacitance has been linked to fate in many lineages (Lee et al., 2018a). Analysis of hematopoietic stem cells, mesenchymal and adipose-derived stem cells, embryonic and pluripotent stem cells, and neural stem cells by DEP and related techniques has demonstrated fate-specific cell electrophysiological signatures that could be exploited for cell type-specific sorting (Lee et al., 2018a).

3.6. Optimizing label-free hNSPC sorting

We identified several approaches that improved sorting efficacy. Analyzing each population of cells prior to sorting was crucial since it took into account any sources of variability that might affect the separation. Three types of analyses were used prior to sorting: DEP spectra were collected with the 3DEP analyzer and converted to trapping curves, trapping curves were generated using the microwell device, and focusing curves were determined in the HOAPES DEP device. Each of these approaches reliably predicted the appropriate sorting frequency for each set of hNSPCs. Due to the analysis platforms used, trapping curves obtained with the 3DEP analyzer and the microwell device did not incorporate fluid

flow whereas the focusing curves in the HOAPES DEP device did. Since fluid flow is an important element of sorting in HOAPES, the focusing curves were a more reliable means for predicting frequencies for sorting in that device.

The specific characteristics of the two devices used in this study impacted sorting efficacy. The microwell device was easy to use, but its simple design contributed to lower sorting reproducibility. The manual washing steps in the microwell device likely created locally high and uncontrolled fluidic shear forces that interfered with trapping along electrodes due to pDEP. The HOAPES DEP device was designed to remove the need for manual washing and create a consistent and controllable fluid shear force. This resulted in much higher consistency sorting. Since cell separation in the HOAPES DEP device is continuous and does not require “trapping” of cells along electrodes, it reduces cell-cell interaction at electrodes that can disrupt electric field gradients and lower effectiveness of DEP-based sorting. The fluid flow in the HOAPES DEP device can also be manipulated to create the desired balance between induced DEP force attracting cells towards electrodes and fluidic shear forces directing cells along the channel. By loading cells at a concentration of 3×10^6 cells/mL and using a flow rate of 3.5 μL/min, the maximal throughput of the HOAPES device is on the order of 630,000 cells/hour.

A main advantage of the HOAPES DEP device is the ability to generate both enriched and depleted cell populations with a single sort. This yields cell populations with distinct characteristics that are more different from each other than from control, unsorted cell populations. For hNSPCs, we obtained focused and unfocused populations that differed by more than 2-fold in the amount of astrocyte-biased cells (Fig. 6E). The HOAPES DEP device thus introduces new functionality to DEP-based devices used to sort stem cells (Adams et al., 2018; Lee et al., 2018a).

4. Conclusion

Populations of hNSPCs that differ in fate potential also differ in membrane capacitance (Labeed et al., 2011). We show here that isolation of subpopulations of hNSPCs with higher membrane capacitance values selects for astrocyte-biased cells. Thus, label free sorting solely on the basis of cell electrophysiological properties is sufficient to enrich populations of human stem cells linked to specific fates. Designing sorting strategies and devices to optimize isolation of subsets of cells from human stem cells enables enrichment of specific populations of cells to assess their cell biological and therapeutic roles.

Supplementary Material

Refer to Web version on PubMed Central for supplementary material.

Acknowledgements

The authors would like to thank Dr. Philip Schwartz for supplying hNSPCs. This work was supported in part by the National Science Foundation Postdoctoral Research Fellowship in Biology DBI-1612261 (TNGA), University of California Chancellor’s ADVANCE Postdoctoral Fellowship (TNGA), and the California Institute of Regenerative Medicine (CIRM) RB5-07254 (LAF).

References

Adams TNG, Jiang AYL, Vyas PD, Flanagan LA, 2018. Methods 133, 91–103. [PubMed: 28864355]

Adams TNG, Leonard KM, Minerick AR, 2013. Biomicrofluidics 7, 064114.

Adams TNG, Turner PA, Janorkar AV, Zhao F, Minerick AR, 2014. Biomicrofluidics 8, 054109.

Bagnaninchi PO, Drummond N, 2011. Proc. Natl. Acad. Sci. U. S. A 108, 6462–6467. [PubMed: 21464296]

Broche LM, Labeed FH, Hughes MP, 2005. Phys. Med. Biol 50, 2267–2274. [PubMed: 15876666]

Chen CS, Pohl HA, 1974. Ann. N. Y. Acad. Sci 238, 176–185. [PubMed: 4613238]

Choi S, Park JK, 2010. Biomicrofluidics 4, 46503. [PubMed: 21139701]

Flanagan LA, Lu J, Wang L, Marchenko SA, Jeon NL, Lee AP, Monuki ES, 2008. Stem Cells 26, 656–665. [PubMed: 18096719]

Flanagan LA, Rebaza LM, Derzic S, Schwartz PH, Monuki ES, 2006. J. Neurosci. Res 83, 845–856. [PubMed: 16477652]

Fry CH, Salvage SC, Manazza A, Dupont E, Labeed FH, Hughes MP, Jabr RI, 2012. Biophys. J 103, 2287–2294. [PubMed: 23283227]

Garner OB, Baum LG, 2008. Biochem. Soc. Trans 36, 1472–1477. [PubMed: 19021578]

Gascoyne PRC, Shim S, Noshari J, Becker FF, Stemke-Hale K, 2013. Electrophoresis 34, 1042–1050. [PubMed: 23172680]

Hu X, Bessette PH, Qian J, Meinhart CD, Daughtery PS, Soh HT, 2005. Proc. Natl. Acad. Sci 102, 15757–15761. [PubMed: 16236724]

Khoshmanesh K, Nahavandi S, Baratchi S, Mitchell A, Kalantar-zadeh K, 2011. Biosens. Bioelectron 26, 1800–1814. [PubMed: 20933384]

Labeed FH, Lu JT, Mulhall HJ, Marchenko SA, Hoettges KF, Estrada LC, Lee AP, Hughes MP, Flanagan LA, 2011. PLoS One 6 e25458.

Lee AP, Aghaamoo M, Adams TNG, Flanagan LA, 2018a. Current Stem Cell Rep 4, 116–126.

Lee DH, Li X, Jiang A, Lee AP, 2018b. Biomicrofluidics 12, 054104.

Leonard KM, Minerick AR, 2011. Electrophoresis 32, 2512–2522. [PubMed: 21874652]

Lepore AC, Rauck B, Dejea C, Pardo AC, Rao MS, Rothstein JD, Maragakis NJ, 2008. Nat. Neurosci 11, 1294–1301. [PubMed: 18931666]

Lindvall O, Kokaia Z, 2006. Nature 441, 1094–1096. [PubMed: 16810245]

Lu J, Barrios CA, Dickson AR, Nourse JL, Lee AP, Flanagan LA, 2012. Integr Biol 4, 1223–1236.

Martinsen OG, Grimnes S, Schwan HP, 2002. Encyclopedia Surf Colloid Sci 20, 2643–2652.

Nourse JL, Prieto JL, Dickson AR, Lu J, Pathak MM, Tombola F, Demetriou M, Lee AP, Flanagan LA, 2014. Stem Cells 32, 706–716. [PubMed: 24105912]

Paszek MJ, DuFort CC, Rossier O, Bainer R, Mouw JK, Godula K, Hudak JE, Lakins JN, Wijekoon AC, Cassereau L, Rubashkin MG, Magbanua MJ, Thorn KS, Davidson MW, Rugo HS, Park JW, Hammer DA, Giannone G, Bertozzi CR, Weaver VM, 2014. Nature 511, 319–325. [PubMed: 25030168]

Patel S, Showers D, Vedantam P, Tzeng TR, Qian SZ, Xuan XC, 2012. Biomicrofluidics 6, 034102.

Pethig R, 2010. Biomicrofluidics 4, 022811.

Pethig R, Menachery A, Pells S, De Sousa P, 2010. J. Biomed. Biotechnol 2010, 182581.

Pohl HA, 1978. Dielectrophoresis: the Behavior of Neutral Matter in Nonuniform Electric Fields. Cambridge University Press, Cambridge, New York.

Razak MAA, Hoettges KF, Fatoyinbo HO, Labeed FH, Hughes MP, 2013. Biomicrofluidics 7, 064110.

Salmanzadeh A, Davalos RV, 2014. Electrokinetics and rare-cell detection. In: Labeed FH, Fatoyinbo HO (Eds.), Microfluidics in Detection Science: Lab-On-A- Chip Technologies. RSC Publishing, Cambridge, pp. 61–83.

Salmanzadeh A, Elvington ES, Roberts PC, Schmelz EM, Davalos RV, 2013. Integr Biol 5, 843–852.

Salmanzadeh A, Romero L, Shafiee H, Gallo-Villanueva RC, Stremler MA, Cramer SD, Davalos RV, 2012. Lab Chip 12, 182–189. [PubMed: 22068834]

Schwartz PH, Bryant PJ, Fuja TJ, Su H, O'Dowd DK, Klassen H, 2003. J. Neurosci. Res 74, 838–851. [PubMed: 14648588]

Simon MG, Li Y, Arulmoli J, McDonnell LP, Akil A, Nourse JL, Lee AP, Flanagan LA, 2014. Biomicrofluidics 8, 064106.

Song HJ, Rosano JM, Wang Y, Garson CJ, Prabhakarpandian B, Pant K, Klarmann GJ, Perantoni A, Alvarez LM, Lai E, 2015. Lab Chip 15, 1320–1328. [PubMed: 25589423]

Song S, Choi S, 2013. Cytometry 83A, 1034–1040.

Srivastava SK, Daggolu PR, Burgess SC, Minerick AR, 2008. Electrophoresis 29, 5033–5046. [PubMed: 19130588]

Vykoukal DM, Gascoyne PRC, Vykoukal J, 2009. Integr Biol 1, 477–484.

Wang XB, Huang Y, Gascoyne PR, Becker FF, Holzel R, Pethig R, 1994. Biochim. Biophys. Acta 1193, 330–344. [PubMed: 8054355]

Yale AR, Nourse JL, Lee KR, Ahmed SN, Arulmoli J, Jiang AYL, McDonnell LP, Botten GA, Lee AP, Monuki ES, Demetriou M, Flanagan LA, 2018. Stem Cell Rep 11, 869–882.

Yamanaka K, Komine O, 2018. Neurosci. Res 126, 31–38. [PubMed: 29054467]

Yuan SH, Martin J, Elia J, Flippin J, Paramban RI, Hefferan MP, Vidal JG, Mu Y, Killian RL, Isarel MA, Emre N, Marsala S, Marsala M, Gage FH, Goldstein LS, Carson CT, 2011. PLoS One 6, e17540.

Zhao FT, Li J, Shi GX, Liu Y, Zhu LP, 2002. Cell Biol. Int 26, 627–633. [PubMed: 12127942]

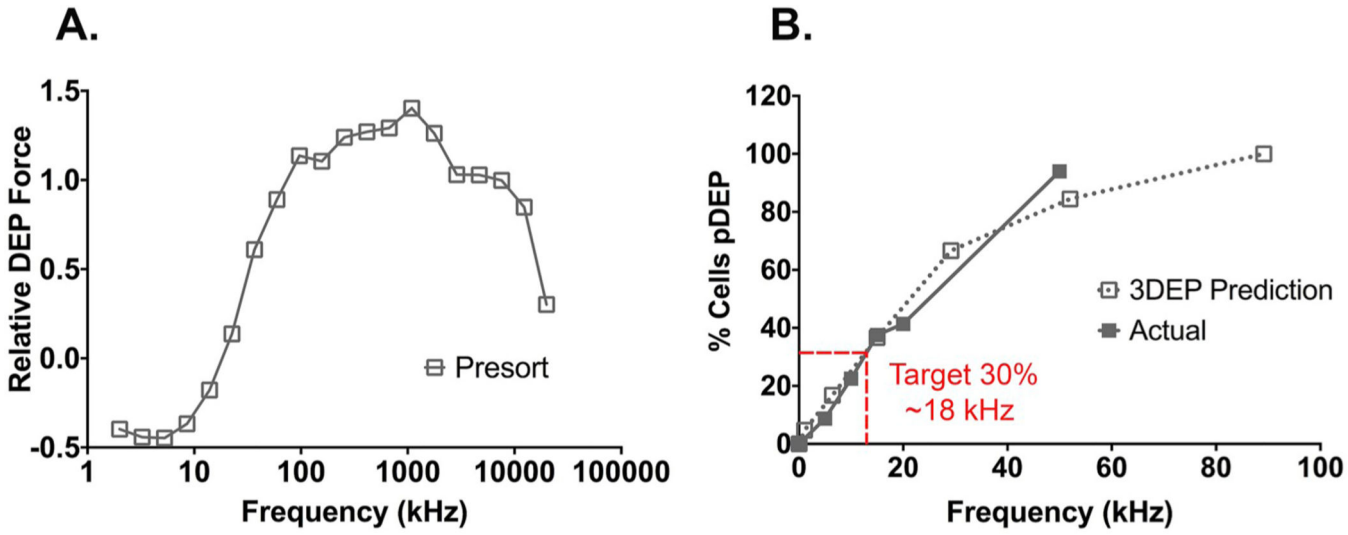

Fig. 1. Rapid prediction of optimal sorting frequency for hNSPCs.

(A) A characteristic 3DEP spectrum for hNSPCs before sorting (presort). (B) The pDEP trapping curve translated from the DEP spectrum (3DEP Prediction) predicts an optimal frequency for enrichment of astrocyte-biased cells (target 30% of cells experiencing pDEP, corresponds to 18 kHz). The 3DEP prediction matches well the actual trapping curve obtained manually with the microwell device (n = 1).

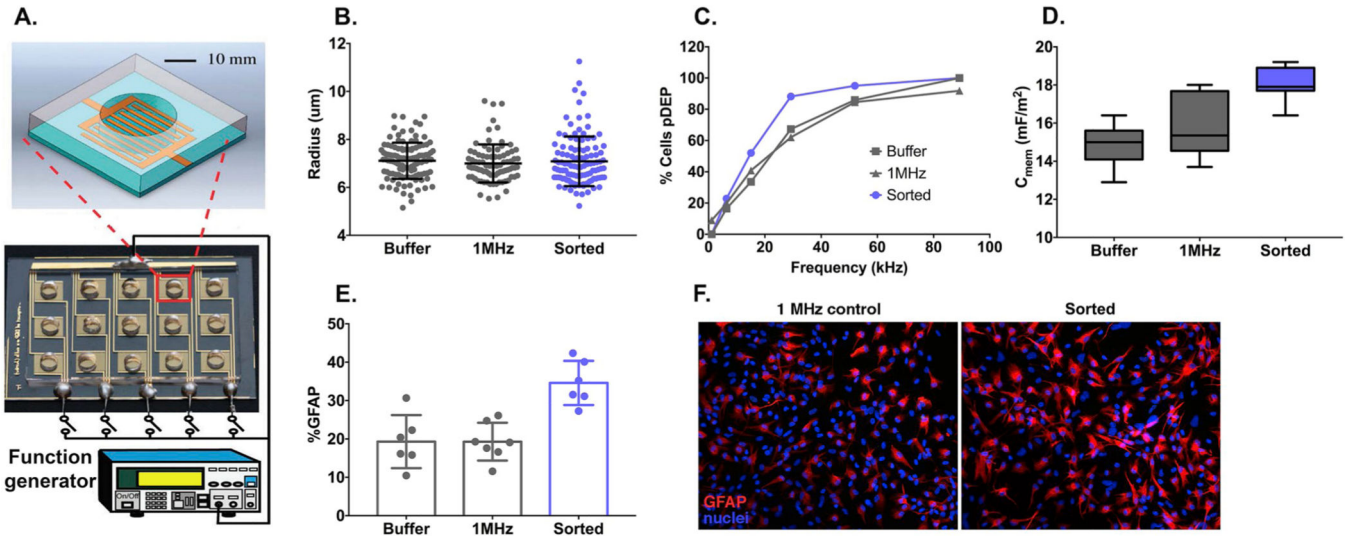

Fig. 2. Astrocyte-biased cells differing in electrophysiological properties but not size were enriched from hNSPCs using a DEP microwell device.

(A) Microwell DEP sorter with interdigitated electrodes on the bottom of the microwell. The microwell is created with PDMS and the entire device contains 15 wells connected to a function generator (3 Vpp applied) (adapted from Lu et al., 2012 with permission from Oxford University Press). (B) Size comparison of sorted cells versus unsorted controls (buffer and 1 MHz, n = 2). (C) Analysis of post-sort trapping curve from 3DEP analyzer of sorted cells compared to buffer and 1 MHz controls (n = 1). (D) There was an increase in the membrane capacitance (C_{mem}) of sorted cells compared to buffer, and 1 MHz controls (n = 2). (E) The percentage of GFAP-positive astrocytes differentiated from sorted cells was higher than that of unsorted controls (n = 2). (F) Images of cells differentiated after sorting and immunostained for the astrocyte marker GFAP show more GFAP-positive astrocytes formed by sorted cells than controls. Error bars indicate the standard deviation.

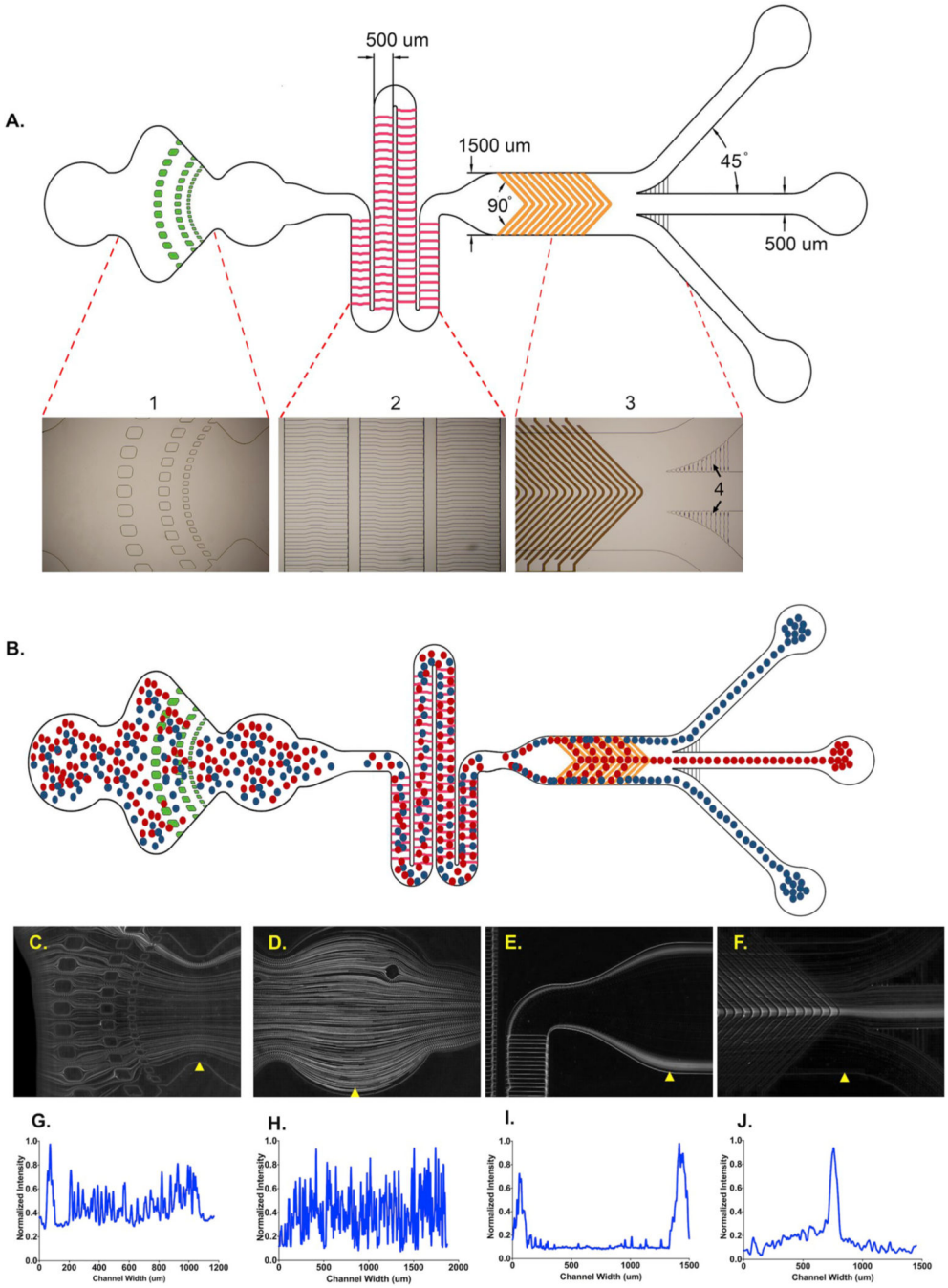

Fig. 3. HOAPES DEP device schematic and operation with cells.

(A) The HOAPES DEP device is composed of three main components: filter (inset 1), sheathless hydrophoretic cell aligner (inset 2), and oblique electrodes (inset 3). The filter is composed of PDMS posts (green) that extend the height of the microchannel (70 μm). The sheathless hydrophoretic cell aligner is composed of a PDMS layer (pink) that is 40 m thick located either on the top or bottom of the microchannel. The electrode region is composed of planar gold electrodes (gold) 50 μm in width, spaced 50 μm apart, and 0.10 μm thick. The end of the channel has 3 outlets with 8 μm microchannel arrays (label 4 in inset 3). (B)

A mixture of cells (red and blue circles) enter the device and flow through the filter (for particle removal), into the cell aligner (pushes cells toward microchannel edges), and then to the electrode region for sorting (cells focused to middle or outer microchannels). (C to F) Traces of hNSPCs moving through the device were generated using Z-projection images of the filter, chamber, sheathless hydrophoretic cell aligner, and electrode regions; white lines show hNSPC trajectories. In the filter and chamber regions the cells are randomly distributed throughout the microchannel (C,D). As the cells exit the sheathless hydrophoretic cell aligner they are focused along the microchannel edges (E). When the DEP electrodes are set to high frequency (in this case, 800 kHz), cells in pDEP are pulled to the center of the channel (F). (G to J) Intensity analysis of the traces shows the distribution of cells across the channel in each region. Random distribution of cells within the device is shown by multiple intensity peaks (G, H), whereas focused cells give defined peaks at the channel edges (I) or center (J). The yellow arrows in C–F indicate channel regions for intensity analyses shown in G-J. (For interpretation of the references to colour in this figure legend, the reader is referred to the Web version of this article.)

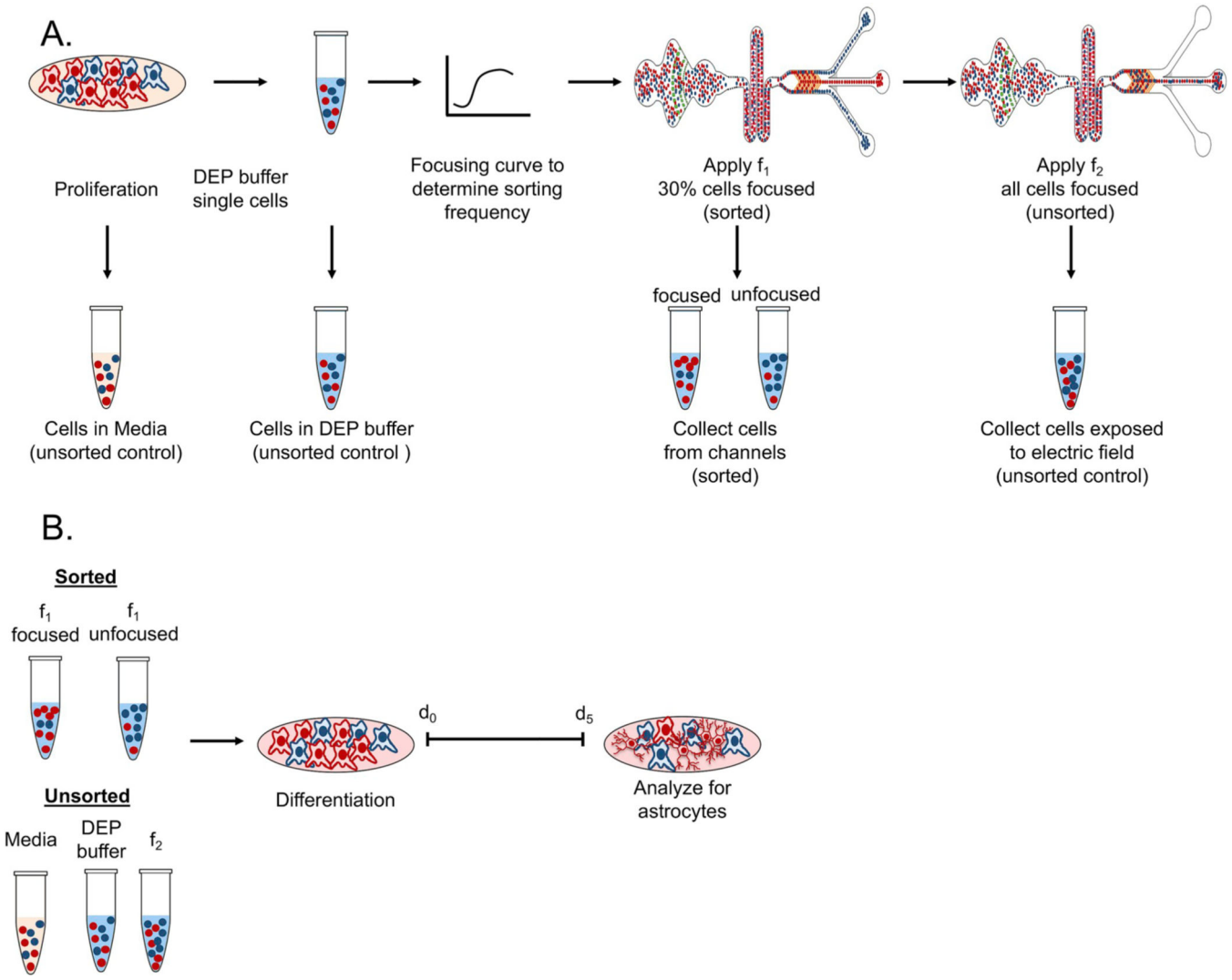

Fig. 4. Sorting experiment workflow for HOAPES DEP device.

(A) Undifferentiated hNSPCs cultured in proliferation media are dissociated to single cells and resuspended in DEP buffer solution. A focusing curve is generated based on the percentage of cells that focus to the middle microchannel. A sorting frequency is selected, f_1, such that 30% of cells focus to the middle microchannel and 70% of cells exit the outer microchannels. A higher frequency, f_2 (1 MHz), is used to collect an unsorted control population of cells to the middle microchannel (exposed to the electric field but not sorted). Additional unsorted controls (downward black arrows) include media and DEP buffer controls. (B) The sorted cells (collected from middle and outer microchannels) along with the unsorted controls (media, DEP buffer, and unsorted exposed to the electric field) are differentiated for 5 days to measure astrocyte differentiation.

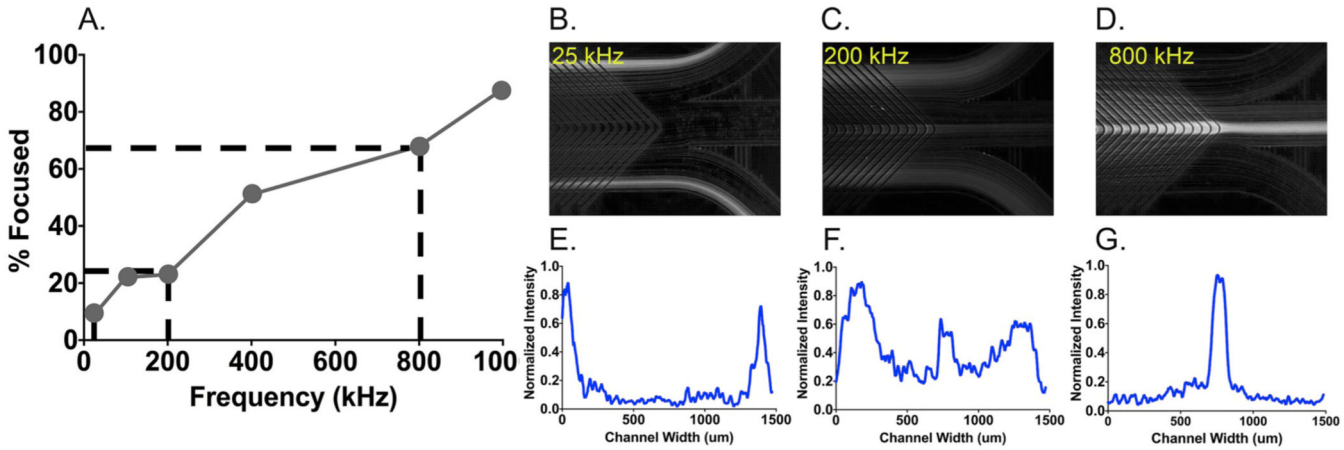

Fig. 5. HOAPES DEP device focuses cells at specific frequencies.

(A) DEP focusing curve for unsorted hNSPCs in the HOAPES DEP device shows % focused (the percentage of cells focused to the middle microchannel of the HOAPES DEP device) as a function of frequency of the applied electric field. The percentage of cells focused to the middle microchannel increases with increasing frequency. HNSPC traces (Z-projection images) show cell trajectories at (B) 25 kHz, (C) 200 kHz, and 800 kHz. At lower frequencies very few cells focus to the middle channel while at higher frequencies more cells focus to the middle channel. (E to G) demonstrates cell location in the channel via intensity analysis.

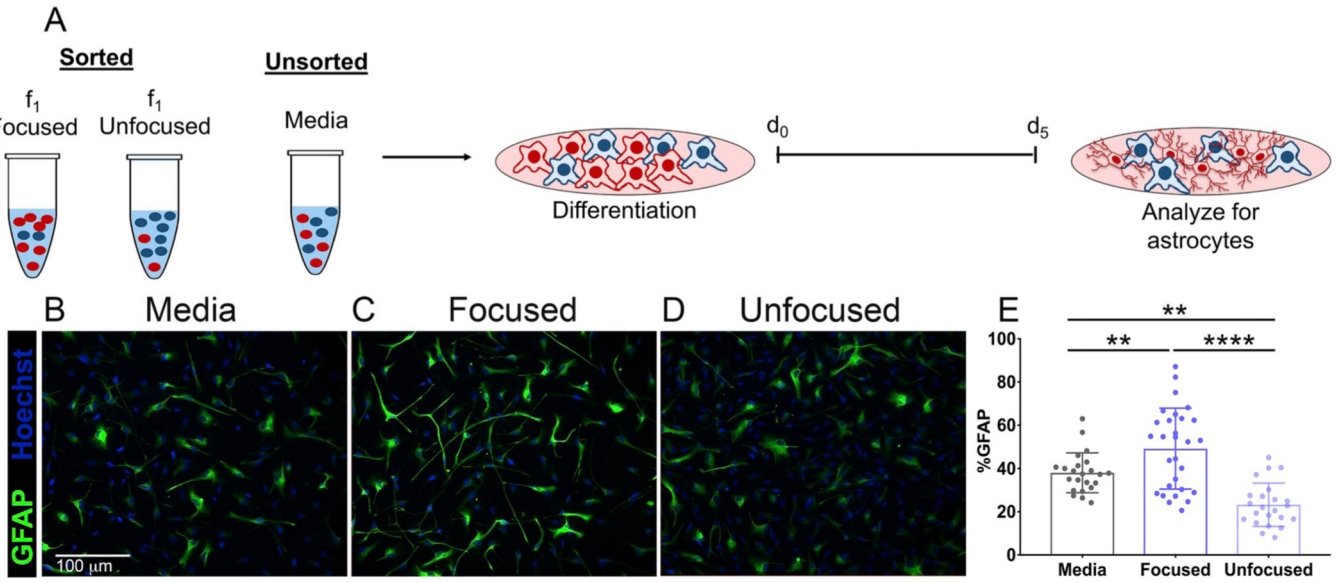

Fig. 6. Enriched and depleted astrocyte-biased populations after sorting hNSPCs with the HOAPES DEP device.

Undifferentiated hNSPCs were sorted in the HOAPES DEP device at f_1 (~30% of cells focused to middle microchannel). (A) The sorted cells collected from middle (focused) and outer (unfocused) channels and the unsorted media control were differentiated for 5 days to assess formation of astrocytes. (B) Unsorted control cells (media control), (C) Focused, and (D) Unfocused cells were differentiated post-sorting to generate astrocytes (detected by GFAP expression, shown in green). Cell nuclei were stained with Hoechst (shown in blue). (E) Quantitation of GFAP-positive cells shows significantly more astrocytes were formed from the focused set of sorted cells (49% GFAP-positive) and fewer from the unfocused cells (23% GFAP-positive)(n = 5). Error bars indicate the standard deviation. (For interpretation of the references to colour in this figure legend, the reader is referred to the Web version of this article.)